

Losses of Tapered Dielectric Slab Waveguides with Axial Variations in Index of Refraction

ROBERT SCARMOZZINO, DRAGAN V. PODLESNIK, MEMBER, IEEE, AND
RICHARD M. OSGOOD, JR., FELLOW, IEEE

Abstract—The effects of varying the index of refraction in the cladding along the length of a tapered dielectric waveguide are calculated using a local normal mode analysis. It is found that in some cases the losses can be reduced by an order of magnitude, even for short tapers whose length is of the order of the guide dimensions.

I. INTRODUCTION

THE POWER losses incurred by a mode incident on a stepped or tapered section of a waveguide have been calculated by a variety of methods [1]–[4]. It was found that the losses are approximately the same for steps or short tapers (independent of the shape of the taper) and that increasing the length of the taper will reduce the losses. In addition, for longer tapers, adjusting the shape of the taper can reduce the losses. However, generally it is assumed that the index of refraction of each region is constant along the taper. Recently [5], a special class of curved waveguide tapers has been explored in which the index of the core varies in a particular way throughout the taper. These structures possess normal modes which propagate without radiation loss; however at a transition between straight and tapered sections losses may still occur. In this paper we follow a different approach, and investigate the effect of arbitrarily varying the index of the cladding along the length of the taper, in the hope of creating a “matched” structure. We find that in some cases we are able to reduce the total losses (including transition) by an order of magnitude, even for short tapers whose length is of the order of the guide dimensions. The technique has other potential applications such as waveguide bends, branches, and couplers.

Our motivation for considering waveguides with index variations along the guide is provided by some recent work [6] in which riblike waveguides were formed in GaAs via a direct-write laser-etching technique. In that work, the lateral confinement in the slab waveguide is provided by the lower effective index of the etched regions. These etched regions effectively form a cladding in the analogous sym-

Manuscript received June 6, 1989; revised August 29, 1989. This work was supported by the National Science Foundation, the Defense Advanced Research Projects Agency, and the Air Force Office of Scientific Research.

The authors are with the Microelectronics Sciences Laboratory and the Center for Telecommunications Research, Columbia University, New York, NY 10027.

IEEE Log Number 8932005.

metric slab waveguide in the lateral direction (see Fig. 1(a)–(c)). The authors point out that by changing the etch depth along the guide, which can be done easily and controllably with their process, the effective index of the cladding may be varied [7] (see Fig. 1(d) and (e)). In order to see whether any benefit can be derived from varying the etch depth along the guide, one must be able to calculate propagation in a structure with longitudinal geometric and index of refraction variations. An appropriate formalism for such calculations is a local normal mode analysis [4], [8], [9].

II. LOCAL NORMAL MODE ANALYSIS

Consider the slab waveguide structure shown in Fig. 1(e). For $z < 0$ or $z > L$, guided modes propagate without loss. However in the “tapered” region $0 \leq z \leq L$, guided modes couple power to other guided modes, as well as to radiation modes. In describing this coupling process, we follow the general treatment and notation of [9]. The transverse fields in the tapered section of the waveguide are expressed as an expansion in local normal modes as follows:

$$\begin{aligned} \mathbf{E}_t &= \sum_{\nu} [c_{\nu}^{(+)}(z) \exp(-i\beta_{\nu}z) + c_{\nu}^{(-)}(z) \exp(+i\beta_{\nu}z)] \hat{\mathbf{E}}_{\nu t} \\ \mathbf{H}_t &= \sum_{\nu} [c_{\nu}^{(+)}(z) \exp(-i\beta_{\nu}z) - c_{\nu}^{(-)}(z) \exp(+i\beta_{\nu}z)] \hat{\mathbf{H}}_{\nu t}. \end{aligned} \quad (1)$$

The summation over ν is a shorthand for a summation over the discrete spectrum (guided modes) and an integration over the continuous spectrum (radiation modes). The summation over forward- and backward-traveling modes has been written explicitly, so that the propagation constants β are assumed to have positive values. The local normal modes ($\hat{\mathbf{E}}_{\nu}$, $\hat{\mathbf{H}}_{\nu}$) are the normal modes of a slab waveguide whose parameters (width, refractive indices) equal those of the tapered section locally. They are functions of the transverse coordinates, as well as of the longitudinal coordinate z through the dependence on the local guide parameters. Insertion of the field expansions into Maxwell's equations results in coupled equations for

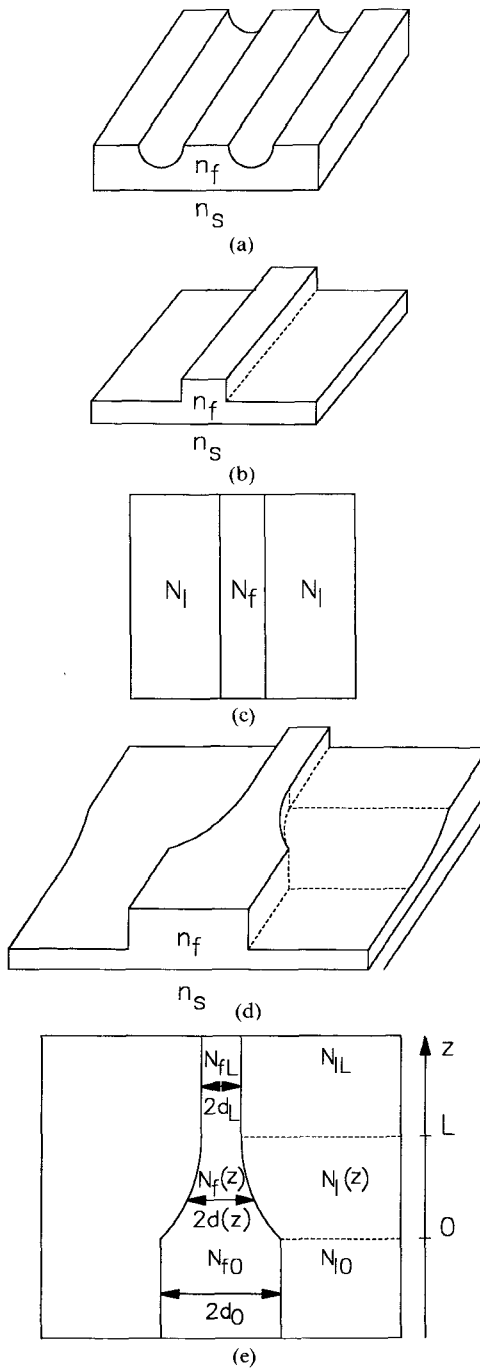


Fig. 1 Sketch of (a) laser fabricated riblike waveguide; (b) conventional rib waveguide which approximates (a); (c) "effective" slab waveguide corresponding to (b); (d) tapered rib waveguide which approximates a tapered laser fabricated riblike waveguide with variable etch depth; (e) "effective" tapered slab waveguide corresponding to (d) with variable index of refraction in the tapered section.

the mode amplitudes $c_{\mu}^{(p)}$:

$$\frac{dc_{\mu}^{(p)}}{dz} = \sum_{\nu} \left\{ R_{\mu\nu}^{(p,+)} c_{\nu}^{(+)} \exp \left[i \int^z (p\beta_{\mu} - \beta_{\nu}) dz' \right] \right. \\ \left. + R_{\mu\nu}^{(p,-)} c_{\nu}^{(-)} \exp \left[i \int^z (p\beta_{\mu} + \beta_{\nu}) dz' \right] \right\}. \quad (2)$$

Providing that the propagation constants are real, which applies in our case, the coupling coefficients $R_{\mu\nu}^{(p,q)}$ can be

expressed as [9]

$$R_{\mu\nu}^{(p,q)}(z) = \frac{p\omega\epsilon_0}{4(p\beta_{\mu} - q\beta_{\nu})} \int_{S(z)} \hat{E}_{\mu}^* \cdot \hat{E}_{\nu} \frac{\partial N^2}{\partial z} dA. \quad (3)$$

Here the integration is over the transverse cross section at z , $S(z)$. The function $N(x, y, z)$ is the refractive index profile in the taper.

The solution of the system of equations (2) requires the specification of each mode amplitude at one or the other end of the taper (i.e., at $z = 0$ or $z = L$). For our calculation we will assume that only one guided mode can exist all along the taper. We consider that the forward-traveling guided mode is incident on the left with unit amplitude, and that all other modes are incident on the taper (at $z = 0$ for forward modes, and $z = L$ for backward modes) with zero amplitude, i.e.,

$$\begin{aligned} c_i^{(+)}(0) &= 1 & c_i^{(-)}(L) &= 0 \\ c_{\mu}^{(+)}(0) &= 0 & c_{\mu}^{(-)}(L) &= 0. \end{aligned} \quad (4)$$

We wish to calculate the power lost from the incident guided mode to the reflected guided mode and to the radiation modes, which is given by

$$\frac{\Delta P}{P} = |c_i^{(-)}(0)|^2 + \int |c_{\rho}^{(-)}(0)|^2 d\rho + \int |c_{\rho}^{(+)}(L)|^2 d\rho. \quad (5)$$

The index ρ , used here to label the radiation modes, will become clear when we introduce explicit expressions for the local normal modes. The range of integration will also be considered later.

In order to render the system of equations (2) tractable, we perform a perturbation calculation and assume that, to first order,

$$\begin{aligned} c_i^{(+)}(z) &\approx \text{constant} \\ c_{\mu}^{(\rho)}(z) &\ll c_i^{(+)}(z), \quad (p, \mu) \neq (+, i). \end{aligned} \quad (6)$$

This corresponds to saying that the incident mode does not lose significant power to the other modes over the length of the taper, which is the case of interest. Equation (2) becomes

$$\frac{dc_{\mu}^{(\rho)}}{dz} = R_{\mu i}^{(p,+)} \exp \left[i \int^z (p\beta_{\mu} - \beta_i) dz' \right]. \quad (7)$$

This can be integrated to yield

$$c_{\mu}^{(\rho)}(z) = \int_{z^*}^z R_{\mu i}^{(p,+)} \exp \left[i \int^{z'} (p\beta_{\mu} - \beta_i) dz'' \right] dz' \quad (8)$$

where z^* is the location at which the mode is "born," i.e., the location such that the mode has zero amplitude beyond z^* (before z^* for forward modes, and after z^* for backward modes). For the reflected guided mode we have from (4) that $z^* = L$ in all cases. For the case of constant (in z) indices of refraction, we have from (4) that $z^* = 0$ for forward radiation modes, and $z^* = L$ for backward radiation modes. For the case of variable index, it can happen that, for example, a forward radiation mode can exist on the right, but not on the left, and so must be born

somewhere in the middle. The location z^* , which depends on the mode μ , was introduced to handle this type of situation. Note that for the purposes of calculating the power loss, the precise phase of $c_\mu^{(p)}(z)$ is unimportant as it cancels out in (5). Therefore the lower limit for the phase integral can be chosen arbitrarily, provided it is within the range of the mode's existence.

For simplicity we will restrict our calculation to the case of even TE modes propagating in a symmetric slab waveguide in which we assume $\partial/\partial y = 0$. We denote the half-width of the guide by d , and the indices of refraction in the core and cladding are denoted by N_f and N_l respectively. The normal modes for this structure are well known, and are presented here for completeness. The even TE guided modes are

$$\begin{aligned} E_y^g(x) &= A_g \frac{\cos \kappa x}{\cos \kappa d}, \quad x \leq d \\ E_y^g(x) &= A_g \exp[-\gamma(x-d)], \quad x \geq d \\ \kappa^2 &\equiv k^2 N_f^2 - \beta^2 \\ -\gamma^2 &\equiv k^2 N_l^2 - \beta^2 \\ A_g^2 &\equiv \frac{2\omega\mu_0}{\beta} \frac{\gamma}{1+\gamma d} \frac{\kappa^2}{\kappa^2 + \gamma^2}. \end{aligned} \quad (9)$$

The dispersion relation for the guided mode propagation constant is

$$\tan \kappa d = \gamma/\kappa. \quad (10)$$

The even TE radiation modes are

$$\begin{aligned} E_y^r(x) &= A_r \frac{\cos \sigma x}{\cos \sigma d}, \quad x \leq d \\ E_y^r(x) &= A_r \left[\cos \rho(x-d) - \frac{\sigma}{\rho} \frac{\sin \sigma d}{\cos \sigma d} \sin \rho(x-d) \right], \quad x \geq d \\ \sigma^2 &\equiv k^2 N_f^2 - \beta^2 \\ \rho^2 &\equiv k^2 N_l^2 - \beta^2 \\ A_r^2 &\equiv \frac{2\omega\mu_0}{\pi\beta} \frac{\rho^2}{\rho^2 + \sigma^2 \tan^2 \sigma d}. \end{aligned} \quad (11)$$

Note that these expressions have been written for $x \geq 0$, and are to be extended as even functions of x .

The normal modes expressed by (9)–(11) are functions of the transverse coordinate x . They are transformed into local normal modes depending on both x and z by allowing the guide parameters d , N_f , and N_l that appear in (9)–(11) to depend on z . When this is the case we may write the following expression for the index of refraction in the taper:

$$\begin{aligned} N(x, z)^2 &= N_f(z)^2 [1 - u(x - d(z))] \\ &\quad + N_l(z)^2 u(x - d(z)). \end{aligned} \quad (12)$$

Here $u(z)$ is the unit step function. We may differentiate

this to obtain

$$\begin{aligned} \frac{\partial N^2}{\partial z} &= (N_f^2 - N_l^2) d'(z) \delta(x - d(z)) + [N_f^2]' \\ &\quad \cdot [1 - u(x - d(z))] + [N_l^2]' u(x - d(z)). \end{aligned} \quad (13)$$

Here the primes represent derivatives with respect to z .

We now have all that we need to calculate the coupling coefficients from (3). We will assume for simplicity that only d and N_l depend on z , as this is the case for the riblike waveguides with variable etch depth. The result of this straightforward calculation is

$$\begin{aligned} R_u^{(-, +)} &= \frac{1}{2} \frac{\kappa_i^2}{\beta_i^2} \frac{\gamma_i}{1 + \gamma_i d} F_g(z) \\ F_g(z) &= d'(z) + \frac{1}{2\gamma_i} \frac{[N_l^2]'}{N_f^2 - N_l^2} \end{aligned} \quad (14)$$

$$\begin{aligned} R_{\rho i}^{(p, +)} &= \frac{\kappa_i}{\beta - p\beta_i} \\ &\quad \cdot \left\{ \frac{k^2 (N_f^2 - N_l^2)}{\pi\beta\beta_i} \frac{\gamma_i}{1 + \gamma_i d} \frac{\rho^2}{\rho^2 + \sigma^2 \tan^2 \sigma d} \right\}^{1/2} F_r(z) \end{aligned}$$

$$F_r(z) = d'(z) + \frac{\gamma_i + \sigma \tan \sigma d}{\gamma_i^2 + \rho^2} \frac{[N_l^2]'}{N_f^2 - N_l^2}. \quad (15)$$

In these expressions note that (in addition to d and N_l) β_i , κ_i , and γ_i depend on z , and β and σ depend on both ρ and z . The radiation modes are labeled by ρ , which is constant in z .

With expressions for the coupling coefficients, we can evaluate the mode amplitudes from (8). These are inserted into (5) to calculate the power loss. We must now consider two related issues: the evaluation of z^* for a particular mode ρ , and the range of integration for ρ . In general, at a given z there exist radiation modes for $0 \leq \rho \leq \infty$; however modes with $\rho > kN_l(z)$ are evanescent and carry no power. Therefore to obtain the relative power in the forward or backward modes at a given z one must calculate

$$\frac{P^{(p)}(z)}{P} = \int_0^{kN_l(z)} |c_\rho^{(p)}(z)|^2 d\rho. \quad (16)$$

In evaluating z^* , we consider, for example, that $N_l(z)$ increases monotonically from a minimum at $z = 0$ to a maximum at $z = L$. For forward-traveling modes we need to evaluate $c_\rho^{(+)}(L)$. Forward modes with $0 \leq \rho \leq kN_l^{\min}$ can exist throughout the taper, and by (4) were born at $z = 0$; therefore we must use $z^* = 0$ in (8). However at $z = L$ forward modes can also exist in the range $kN_l^{\min} \leq \rho \leq kN_l^{\max}$. For ρ in this range, a mode can exist only for $z \geq z^*$, where z^* satisfies $kN_l(z^*) = \rho$. Considering the backward-traveling modes, we must compute $c_\rho^{(-)}(0)$. All the backward modes at $z = 0$ have $0 \leq \rho \leq kN_l^{\min}$ and can exist throughout the taper; therefore for these modes $z^* = L$. However for ρ in the range $kN_l^{\min} \leq \rho \leq kN_l^{\max}$, backward modes will be born at $z^* = L$, and will "die" (i.e., will be converted to other modes) before they reach $z = 0$.

Regardless of their fate, these modes will draw power from the incident mode. This additional power loss can be included in (5) if we extend the range of integration for backward modes to $\rho = kN_l^{\max}$ and replace $c_\rho^{(-)}(0)$ with $c_\rho^{(-)}(z^\dagger)$, where z^\dagger satisfies $kN_l(z^\dagger) = \rho$. In summary, for monotonically increasing $N_l(z)$, we evaluate the power loss from

$$\frac{\Delta P}{P} = |c_l^{(-)}(z^\dagger)|^2 + \int_0^{kN_l^{\max}} |c_\rho^{(-)}(z^\dagger)|^2 d\rho + \int_0^{kN_l^{\max}} |c_\rho^{(+)}(z^\dagger)|^2 d\rho \quad (17a)$$

where for the reflected guided mode $z^* = L$ and $z^\dagger = 0$. For the backward radiation modes,

$$\begin{aligned} z^* = L & \quad z^\dagger = 0, & 0 \leq \rho \leq kN_l^{\min} \\ z^* = L & \quad z^\dagger: kN_l(z^\dagger) = \rho, & kN_l^{\min} \leq \rho \leq kN_l^{\max} \end{aligned} \quad (17b)$$

and for the forward radiation modes

$$\begin{aligned} z^* = 0 & \quad z^\dagger = L, & 0 \leq \rho \leq kN_l^{\min} \\ z^*: kN_l(z^*) = \rho & \quad z^\dagger = L, & kN_l^{\min} \leq \rho \leq kN_l^{\max}. \end{aligned} \quad (17c)$$

The case for monotonically decreasing $N_l(z)$ can be analyzed similarly.

III. NUMERICAL RESULTS

Given the taper parameters $d(z)$, $N_l(z)$, and N_f , we are now in a position to calculate the mode amplitudes and losses by numerical integration of (8) and (17) (see the Appendix for details).

In the calculations that follow, we assume the following form for the shape of the taper:

$$d(z) = d_0 + (d_L - d_0) \frac{1 - \exp(-bz/L)}{1 - \exp(-b)}. \quad (18)$$

Here d_0 and d_L are the guide half-widths on the left and right of the taper, L is the length of the taper, and b is a parameter controlling the shape of the taper. This form was chosen to allow any easy transition from a linear taper ($b \rightarrow 0$) to an exponential taper of the type considered in [3].

Before exploring variable tapers, we will consider some properties of losses in simple linear tapers. Fig. 2 shows the spectrum of radiation losses for a typical linear taper. It is more interesting to consider the spectrum versus β instead of ρ ; therefore we have plotted $|c_\rho|^2(\beta/\rho)$ versus β , which includes the appropriate factor from the change of variables. Note also that in the figure the backward-traveling modes are plotted as having negative β . We see from the figure that the power lost to the forward radiation modes is much greater than that lost to the backward modes. In addition, the maximum in the spectrum occurs for β near, but not nearest, β_i .

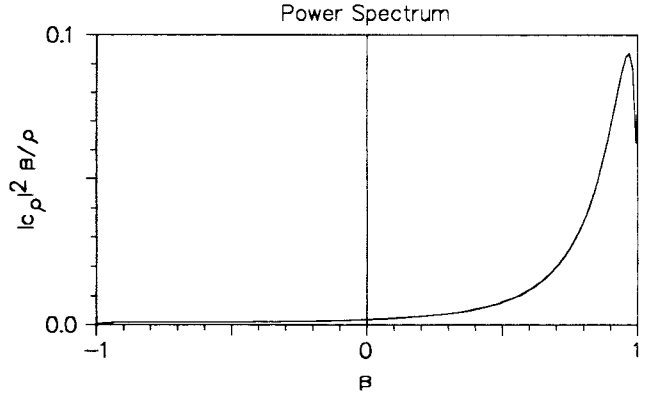


Fig. 2. Spectrum of radiation losses for a typical linear taper. Here $kd_0 = 1$, $d_L/d_0 = 0.5$, $L/d_0 = 1$, $N_f = 1.5$, and $N_l = 1.0$.

Following [3], we calculate the losses as a function of the length of the taper. Fig. 3 shows the result of this calculation, where the individual components of the loss have been plotted separately. We can see that in general, the power lost to the forward radiation modes dominates that lost to the backward radiation modes and to the reflected guided mode. In addition, the power lost to the reflected guided mode can be comparable to that lost in the backward radiation modes. Also note that the reflected power exhibits a smooth oscillatory behavior with respect to L/d_0 , which when plotted on a linear scale turns out to be periodic in L/d_0 with period $\Delta L/d_0 \approx 2.63$.

Next we consider the case of constant N_l , and see what can be done by varying the shape of the taper alone. The parameter b in (18) was varied so as to minimize the total losses at $L/d_0 = 20$ ($b = 1.7$). The total losses for this “optimal” exponential taper were calculated as a function of L/d_0 , and are plotted in Fig. 4, along with results for the linear taper. We see that (as observed in [3] for round waveguides) for long tapers, the exponential taper yields a reduction in the losses over the linear taper. However, for short tapers no benefit is derived from adjusting the shape of the taper.

Note that there is a pronounced kink in the power loss curve for the exponential taper at $L/d_0 \approx 30$ (see Fig. 4), the origin of which is unknown. It does not appear to be the result of numerical error, as this was carefully checked. It is also not due to a minimum in the reflected power (see Fig. 3), as that is a small component of the total loss. It is possible that the choice of b is not optimal for all L/d_0 , leading to a dip near $L/d_0 = 20$, at which the losses were minimized. However a less pronounced kink also appears in the simple linear taper, for which this explanation does not apply, and a dip at $L/d_0 \approx 30$ also occurs for the variable index taper (see following discussion), which was optimized at $L/d_0 = 1$; therefore the cause of these kinks is likely to be something other than nonglobal minimization.

As an aside, note that to obtain a reduction in losses, the parameter b in (18) had to be positive, so that the taper had its largest slope at the wide end, where β_i is maximum. In [3] the author explains why this is so, apparently in general. However, it turns out that for larger kd_0 (beyond

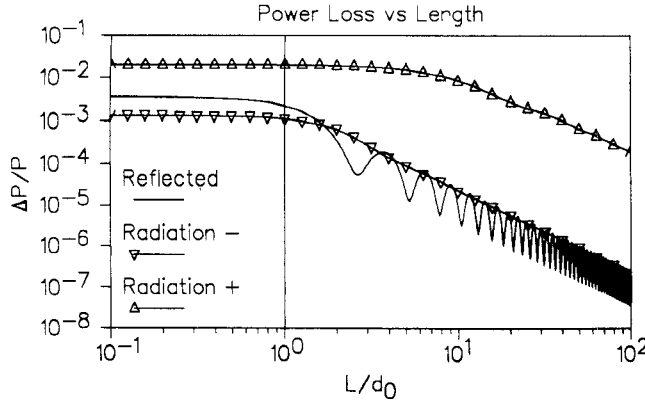


Fig. 3. Power loss into the reflected guided mode, and backward and forward radiation modes, versus length of taper. Here $kd_0 = 1$, $d_L/d_0 = 0.5$, $N_f = 1.5$, and $N_l = 1.0$.

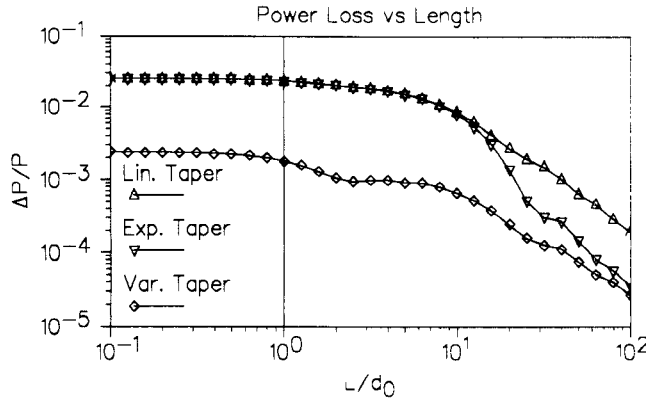


Fig. 4. Total power loss versus taper length for linear, exponential, and variable index tapers. Here $kd_0 = 1$, $d_L/d_0 = 0.5$, $N_f = 1.5$, and $N_l = 1.0$. For the exponential taper, $b = 1.7$. For the variable index taper, $\alpha_0 = 0.31$, $N_{l0} = 1.0$, and $N_{lL} = 1.086$.

the minimum in a $\Delta P/P$ versus kd_0 curve), to achieve a reduction in losses the appropriate sign of b is negative.

Now we allow N_l to depend on z and see what benefit can be derived from this. What form should $N_l(z)$ take so as to minimize the total losses? One idea would be to let $N_l(z)$ be such that the propagation constant of the incident mode, $\beta_i(z)$, is constant in z . Then the taper would be "matched" to the incident mode. It turns out that for this type of taper, (14) for $R_u^{(-,+)}$ vanishes, so that there is no reflected guided mode as we expected. However this leads to radiation losses which are higher than for the case of constant $N_l(z)$. Instead, we try to "minimize" both the $F_g(z)$ and $F_r(z)$ functions in (14) and (15) simultaneously. To do this we write the F functions in the form

$$F(z) = d'(z) + \frac{1}{\alpha(N_l(z))} \frac{[N_l^2]'}{N_f^2 - N_l^2}. \quad (19)$$

Given $d(z)$, if we require $F(z)$ to be identically zero, this becomes a nonlinear differential equation for $N_l(z)$, which, in general, will not have the same solution for two different α 's. Therefore we cannot simultaneously eliminate both the reflected and radiation modes. However, if we choose α to be a constant (in z) parameter, then we can

solve for $N_l(z)$ and then vary α so as to minimize the total losses with respect to this class of functions. When $F = 0$, $\alpha(z) = \alpha_0 = \text{constant}$, (19) can be integrated to yield

$$N_l(z)^2 = N_f^2 - (N_f^2 - N_l(0)^2) \exp [\alpha_0(d(z) - d(0))]. \quad (20)$$

With the above form for $N_l(z)$, a linear taper for $d(z)$, and α_0 chosen so as to minimize the losses at $L/d_0 = 1$ ($\alpha_0 = 0.31$), the losses versus L/d_0 were calculated and are plotted in Fig. 4, along with the results for the constant index linear and exponential tapers. We see from the figure that even for short tapers, where adjusting only the shape of the taper yields no improvement, over an order of magnitude reduction in losses can be achieved with the variable index taper. To achieve the same level of losses as at $L/d_0 = 1$, the linear taper would have to be more than 30 times as long. Therefore a great economy in space can be achieved by using variable index tapers in integrated optics circuits. Note that for large L/d_0 the improvement over the linear taper is not as great and that in fact, for large enough L/d_0 , the losses for the exponential taper seem to approach those for the variable index taper. This is due to our choice of α_0 , which minimizes the losses at $L/d_0 = 1$. However, by choosing α_0 appropriately one can minimize the losses at any desired taper length. For example, at $L/d_0 = 100$ the losses for the variable index taper can be further reduced (from those in Fig. 4) to 0.0014 percent by using $\alpha_0 = 0.26$. These losses are 2.5 times less than those for the exponential taper at this length. By combining the exponential taper shape with the variable index profile, it is possible to obtain losses more than 20 times less than with the exponential taper alone ($b = 1.7$, $\alpha_0 = 0.25$, losses = 0.00028 percent).

An interesting point about the variable index taper is that with an optimal choice for α_0 , the power lost to the reflected guided mode is comparable to that lost in the forward radiation modes. In fact, the dip in the variable index taper loss curve occurring at $L/d_0 \approx 2-3$ (see Fig. 4) is due to the reflected power going through a minimum in L/d_0 (see, e.g., Fig. 3). For larger L/d_0 the reflected power is much smaller than the forward radiated power, and has negligible effect on the total losses displayed in Fig. 4.

The foregoing discussion demonstrates the utility of variable index tapers in slab waveguides. We now discuss the application of this concept to the laser-fabricated rib-like waveguides studied in [6] and [7]. A typical laser-fabricated guide might have $k = 4.064 \mu\text{m}^{-1}$, $d_0 = 1 \mu\text{m}$, $N_f = 3.358$, and $N_l = 3.273$ (corresponding to an air/GaAs/Al_{0.3}Ga_{0.7}As slab waveguide with GaAs thickness $h_0 = 2 \mu\text{m}$, refractive indices [10] $n_{\text{air}} = 1$, $n_{\text{GaAs}} = 3.375$, $n_{\text{AlGaAs}} = 3.189$, and trench edges spaced 2 μm apart and etched to a depth of 1.39 μm). A simple linear taper in such a guide with $d_L/d_0 = 0.5$ and $L/d_0 = 1$ would have total losses of ≈ 4.8 percent. If the etch depth at the narrow end of the taper is decreased to 0.97 μm , corresponding to $N_l = 3.325$, and is tapered from 1.39 μm ,

corresponding to $N_f = 3.273$ according to (20) with $\alpha_0 = 1.9$, the resulting variable index taper would have total losses of ≈ 1.7 percent, yielding a factor of 3 improvement.

There is one caveat which must be discussed in connection with this idea of varying the index of refraction along the taper in order to reduce the losses. It was brought to our attention [11] that the higher index of refraction at the narrow end of the taper has the effect of broadening the mode's lateral profile. Depending on the application, the reduction in physical mode size may be more important than the reduction in geometric size of the taper. We can define the mode size, for example, by the half-width within which 80 percent of the power is carried. For the example guides discussed in the previous paragraph, the mode size at the "narrow" end of the variable index taper is 58 percent larger than that for the constant index taper, and in fact is slightly larger than the mode size at the "wide" end of the taper. However, recall that the loss was improved by a factor of 3. If we characterize a good taper by a low product of loss with mode size, then the variable index taper is still better than the constant index taper by about a factor of 2.

When the taper application is such that the mode size is important, it would be desirable to fix the output mode size at the desired value (equivalently, fix the index at the end of the taper) and then attempt to minimize the loss. This can be accomplished if we increase our freedom in the choice of α and let $\alpha(z) = \alpha_0 + \delta z$. With a linear taper for $d(z)$, and the above form for α , (20) is replaced by

$$N_f(z)^2 = N_f^2 - (N_f^2 - N_f(0)^2) \cdot \exp \left[\left(\alpha_0 z + \frac{1}{2} \delta z^2 \right) (d_L - d_0) / L \right]. \quad (21)$$

For a given α_0 , δ can be chosen to obtain the desired index $N_f(L)$ at the end of the taper; then α_0 can be varied to minimize the losses.

Before concluding, we would like to mention another potential application of variable index tapers which follows immediately from the local normal mode analysis. Suppose that it is desired to make a taper from a double-mode guide to a single-mode guide (or vice versa), and that the radiation losses are deemed unimportant, but coupling between the guided modes is still a problem. By a suitable choice of index profile, it is possible to make the coupling between the two guided modes identically zero, so that the output of the taper contains the unperturbed (except for radiation losses) single mode.

IV. CONCLUSION

The effects of varying the index of refraction in the cladding along the length of a tapered waveguide have been calculated. It was found that in some cases (e.g., $kd_0 = 1$, $N_f = 1.5$, $N_l = 1.0$, 2-to-1 taper) the losses can be reduced by an order of magnitude, even for short tapers whose length is of the order of the guide dimensions. This technique has several other potential uses, including waveguide bends, branches, and couplers. The application of

this variable index waveguide concept is currently being pursued for these other structures.

APPENDIX

The evaluation of the mode amplitudes via (8) requires two nested integrations. In addition, for variable index tapers the integrand in (8) can be singular at one of the endpoints. Although the singularity is integrable, a numerical integration using an open formula can be time consuming, especially if a nonadaptive procedure is employed. It turns out to be more efficient to change variables in (7) and integrate the resulting ODE directly via an adaptive numerical method. The singularity can be dealt with by starting the integration slightly away from the singular point, and by deriving an analytical expression for the proper initial value there.

We can transform (7) into a more convenient form by letting $c_\mu^{(p)} = a_\mu^{(p)} \exp[i \int^z p \beta_\mu dz']$, which results in

$$\frac{da_\mu^{(p)}}{dz} + ip\beta_\mu a_\mu^{(p)} = R_{\mu i}^{(p, +)} a_i^{(+)} \equiv Q_\mu^{(p)} \quad (A1a)$$

$$a_i^{(+)} = \exp \left[-i \int^z \beta_i dz' \right]. \quad (A1b)$$

The phase integral in (A1b) can be evaluated and tabulated once and is independent of the mode μ , so the evaluation of $a_\mu^{(p)}$ from (A1a) requires a single integration of the ODE, as opposed to the two nested integrations in (8) required to evaluate $c_\mu^{(p)}$. The mode amplitudes $c_\mu^{(p)}$ and $a_\mu^{(p)}$ differ only by a phase factor; therefore in evaluating the power loss via (17) we can simply replace $c_\mu^{(p)}$ by $a_\mu^{(p)}$.

When the right-hand side of (A1a) is singular at the starting point of integration z_0 , we write an analytic solution for (A1a) similar to (8), and expand it around z_0 to leading order in Δz . Dropping the μ , (p) notation for simplicity, and assuming $a(z_0) = 0$, the leading order solution for a is

$$a(z_0 + \Delta z) = \int_{z_0}^{z_0 + \Delta z} Q(z') dz'.$$

If the singularity in $Q(z)$ goes like $(z - z_0)^{-q}$, this can easily be integrated to yield

$$a(z_0 + \Delta z) = \frac{1}{1 - q} Q(z_0 + \Delta z) \Delta z.$$

For our particular choice of functions, $q = 1/4$; therefore the ODE in (A1a) should be integrated from $z_0 + \Delta z$ with the initial value

$$a(z_0 + \Delta z) = \frac{4}{3} Q(z_0 + \Delta z) \Delta z. \quad (A2)$$

Similar reasoning yields the procedure for dealing with singularities at the endpoint of integration.

ACKNOWLEDGMENT

The authors would like to thank P. Diamant and D. Marcuse for their insightful comments. They are also

grateful to A. E. Willner for initiating their interest in laser-fabricated waveguides.

REFERENCES

- [1] D. Marcuse, *Bell Syst. Tech. J.*, vol. 48, p. 3177, 1969.
- [2] —, *Bell Syst. Tech. J.*, vol. 49, p. 273, 1970.
- [3] —, *Bell Syst. Tech. J.*, vol. 49, p. 1665, 1970.
- [4] A. W. Snyder, *IEEE Trans. Microwave Theory Tech.*, vol. MTT-18, p. 383, 1970.
- [5] E. A. J. Marcatili, *IEEE J. Quantum Electron.* vol. QE-21, p. 307, 1985.
- [6] A. E. Willner, M. N. Ruberto, D. J. Blumenthal, D. V. Podlesnik, and R. M. Osgood, Jr., *Appl. Phys. Lett.*, vol. 54, no. 19, p. 1839, 1989.
- [7] R. Scarmozzino, D. V. Podlesnik, A. E. Willner and R. M. Osgood, Jr., *Appl. Opt.*, vol. 28, Dec. 15, 1989.
- [8] V. V. Shevchenko, *Continuous Transitions in Open Waveguides*. Boulder, CO: Golem Press, 1971.
- [9] D. Marcuse, *Theory of Dielectric Optical Waveguides*. New York: Academic Press, 1974.
- [10] S. Adachi, *J. Appl. Phys.*, vol. 58, p. R1, 1985.
- [11] D. Marcuse, private communication.

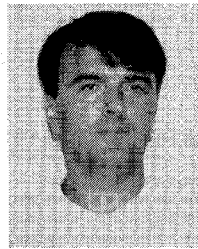
♦



Robert Scarmozzino was born in New York, NY, on July 12, 1961. He received the B.S. and M.S. degrees from the Columbia University School of Engineering and Applied Science in 1982 and 1983 and the Ph.D. degree from the Columbia University Graduate School of Arts and Sciences in 1987, all in applied physics. His graduate research was in the area of plasma physics, and primarily consisted of an experimental and theoretical study of collisionless trapped particle instabilities.

Since 1987, he has been engaged in research at the Columbia University Microelectronics Sciences Laboratory in a variety of applied physics topics related to laser-induced semiconductor processing. These include experiments with, and the modeling of, materials deposition and etching, process diagnostics, and integrated optics components.

Dr. Scarmozzino is a member of the American Physical Society, the Materials Research Society, and of Sigma Xi. He is currently an Associate Research Scientist at the Columbia University Microelectronics Sciences Laboratory.



Dragan V. Podlesnik (S'82-M'85) was born in Belgrade, Yugoslavia. He received the Dipl. Eng. degree from the University of Belgrade in 1979 and the M.Phil. and Ph.D. degrees from the Columbia University Graduate School of Arts and Sciences in 1984 and 1986, all in electrical engineering. His graduate research was in the area of laser processing of electronic materials.

Since 1986, he has been a Research Scientist at the Columbia University Microelectronics Sciences Laboratories and the Center for Telecommunications Research. He is currently engaged in basic and applied research in laser processing of optoelectronic devices.

Dr. Podlesnik is a member of the American Physical Society, the Materials Research Society, and the Electrochemical Society.

♦



Richard M. Osgood, Jr. (SM'82-F'87) received the B.S. degree in engineering from the U.S. Military Academy, the M.S. degree in physics from Ohio State University, and the Ph.D. degree in physics from the Massachusetts Institute of Technology.

He is Professor of Electrical Engineering and of Applied Physics at Columbia University in the City of New York. Prior to this appointment, he served on the scientific staff of M.I.T. Lincoln Laboratory, and the U.S.A.F. Materials Laboratory. Throughout his professional career he has performed research in many areas of electrical engineering, physical chemistry, and optical physics. His most extensive research has been in the development of new infrared and ultraviolet lasers, the application of laser-induced chemistry to materials preparation, and optical surface physics and chemistry.

Dr. Osgood is a member of the ACS, OSA, and MRS. He is coeditor of *Applied Physics*. Along with S. R. J. Brueck, he organized the first MRS symposium on Laser Diagnostics and Photochemical Processing. He has served as a consultant to numerous government and industrial organizations, including the DARPA Materials Research Council, the DOE Basic Energy Sciences Advisory Board, and the Los Alamos National Laboratory Chemistry Advisory Board. In October 1983, Dr. Osgood was elected to a three-year term as councillor of the Materials Research Society, and in 1986, he was selected to be an IEEE-CLEOS Distinguished Traveling Lecturer. He is currently Co-Director of the Columbia Radiation Laboratory and Director of the Microelectronics Sciences Laboratories.